

Non-destructive inspection of SiC_f/SiC composites structure

H. Tatlisu¹, F. Hameed¹, A. Hilger², N. Kardjilov², H. Rauch¹

¹ Atomic Institute of the Austrian Universities, Vienna, Austria

² Helmholtz Zentrum Berlin (former Hahn-Meitner Institut), Berlin, Germany

Email contact of main author: tatlisu@ati.ac.at

Abstract

Fiber reinforced ceramic matrix composite is an attractive candidate as a structural material for future fusion power plants because of their light weight, high temperature capability, high strength and toughness. Ceramic matrix composite made of silicon carbide matrix and fibers (SiC_f/SiC) is promising for nuclear and fusion technology due to its excellent radiation resistance, especially exposure to high-energy particles such as neutron, proton, and alpha. However, porosity, which is mainly due to manufacturing process of the SiC_f/SiC composites, is a critical issue in its application in fusion technology. Internal pores mitigate most of the outstanding properties of the SiC_f/SiC composites such as thermal conductivity, high strength and radiation stability. The pores in composites are unavoidable and significantly reduce the life time and performance of the composites under harsh environments.

The aim of the study is to examine the pore structure and alignment between the matrix/fiber bundles and high-temperature induced changes within the SiC_f/SiC composite. By means of non-destructive cold neutron tomography (at Helmholtz Zentrum Berlin) and small angle neutron scattering (at Paul Scherrer Institute, PSI-Villigen) techniques inner microstructure of the composites have been investigated. The cold neutron tomography and small angle neutron scattering techniques have been applied in order to gain complementary information on the microstructure of the SiC_f/SiC composites. After heat treatment of the composites at 1300 °C, 1400 °C and 1500 °C for 5 hours small angle neutron scattering (SANS) measurements have been carried out to understand the structural changes under high-temperature: pore size changes induced by high temperature. Scattering curves have revealed the changes in pore size at elevated temperatures.

1. Introduction

SiC_f/SiC composites developed for fusion technology, gas turbine, aerospace industry and advanced fission applications are currently under study. The appealing properties of a SiC_f/SiC composite are mainly its high strength at elevated temperature, low density, high hardness, light weight, and superior irradiation tolerance make it ideal for the replacement of metals [1-2].

SiC_f/SiC composite is composed of bundles (500-600) of silicon carbide fibers (14 μm diameter of fibers). These bundles were woven three dimensional and embedded in a silicon carbide matrix. SiC_f/SiC composite is manufactured using a chemical vapour infiltration (CVI) method, which is widely used for fabrication of ceramic matrix composite. CVI is an efficient technique to manufacture high quality composite but slow process, and some unavoidable residual porosity is created during this method. The residual porosity within the composite is between 6-10%. Porosity and swelling represent some of the critical technological issues for the use of the ceramic matrix composites, since porosity causes degradation of the thermal conductivity, outstanding mechanical properties and probability radiation stability. Besides, the porosity would be tended to affect importantly the initiation of matrix cracks. Pore sizes can vary over a wide range from micro-, meso- and macropores.

One of the main obstacles to using this composite in the fusion technology and the other applications are the change of porous structure markedly at high temperature. Improvement of efficiency of the SiC_f/SiC composite obligates comprehensive understanding of the pore structure.

Fig. 1 shows a surface analysis on the SiC_f/SiC composite performed by Scanning Electron Microscopy (SEM) method. The inherent pores with different size can be easily seen on the image where large and small pore examples are marked with arrows. Since SEM is a surface scanning method, pores within the composite can not be investigated using this method. In order to visualize the pores, which are located within the composite, neutron imaging and scattering techniques have been implemented.

Small angle neutron scattering (SANS) and neutron tomography are two powerful non-destructive techniques to characterize pore structure in the porous material on the length scale ranging approximately from nanometer to micrometer, respectively. While neutron scattering can give significant information on microstructure of ceramic materials [3], neutron tomography is a useful technique for analysing the macroscopic inner structure with a spatial resolution of up to 100 μm .

In order to analyse temperature induced structural change within the SiC_f/SiC composites, the samples were heat treated at 1300 $^{\circ}\text{C}$, 1400 $^{\circ}\text{C}$ and 1500 $^{\circ}\text{C}$ for 5 hours and the temperature induced pore structure evaluation was followed by means of SANS.

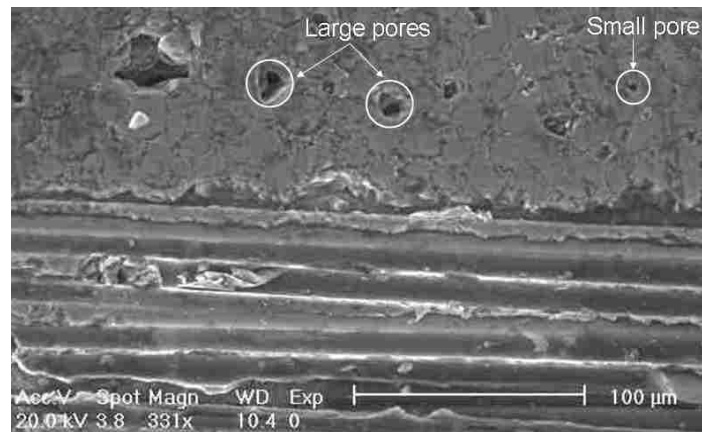


Fig.1. Scanning electron microscopy image from the side of a SiC_f/SiC composite.

2. Experimental

2.1 Small Angle Neutron Scattering (SANS)

SANS experiments were carried out at the SANS-II diffractometer at the Swiss spallation neutron source SINQ at the Paul Scherer Institute (PSI) in Switzerland [4]. The spallation neutron source SINQ at the PSI provides a continuous high flux of neutrons by colliding a proton current of 1.8 mA of 590 MeV on a lead target, are expelled from the lead target nuclei [5].

The principal experimental set-up used for SANS studies is shown in Fig. 2. The SANS instrument is mainly composed of a velocity selector, collimator flight tube, sample holder and neutron detector. The incoming neutron beams are monochromated using a mechanical velocity selector to define the wavelength between 4.5 -20 \AA of the neutron beam even after the collimation is carried out in the six meter long collimator. Experiments were realized with a pinhole collimated beam. Scattering neutrons from a sample were detected at three different sample-detector distance in order to increase accessible the scattering wave vector Q . The

scattering wave vector is defined by the difference of the wave vector of the scattered and incident neutron beam, is given by Eq.(1),

$$|\mathbf{Q}| = Q = (4\pi/\lambda)\sin(\theta/2), \quad (1)$$

where λ is the wavelength incident neutrons, θ is the scattering angle and $Q = k_f - k_i$, k_i is the wave vectors of the incident neutron and k_f is the wave vector of the scattered neutron. The measured absolute intensity is linked to sample and several instrumental specific parameters is given by Eq.(2),

$$I(Q) = I_0 A t T \xi \frac{d\Sigma}{d\Omega}(Q) \Delta\Omega, \quad (2)$$

where I_0 is the incident neutron beam intensity upon sample, A is the surface area of the sample, T is the measured sample transmission, ξ is the detector efficiency, t is the thickness of the sample, $d\Sigma/d\Omega(Q)$ is the macroscopic differential scattering cross section (proportional to the scattering intensity) per unit volume, $\Delta\Omega$ is the solid angle at scattering vector Q . The scattering intensities are recorded as a function of the scattering vector (Q).

The 4.5 Å of neutron wavelength was used for 1.2 and 4 m the sample-to-detector distances and 19.5 Å of neutron wavelength for 6 m sample-to-detector distance. The scattered intensity data were recorded in the accessible scattering wave vector range from $2 \cdot 10^{-3}$ Å to 0.3 Å, covering the structure of a range of lengths ($d = 2\pi/Q$) nearly from 0.15 μm to 10 Å. A two dimensional position sensitive detector (PSD), which is a ^3He area detector of 64 cm in diameter and 128x128 pixels, has been used to collect the scattering neutrons. The detector is used in an evacuated space to avoid air scattering and can be moved continuously from one to six meters away from the sample position.

Information on large scale structure is included in the intensity of the scattered neutrons at small scattering vector or in other words if the sample is measured at a large sample-detector distance, the large porous can be determined. There is an inverse relation between scattering vector and structure.

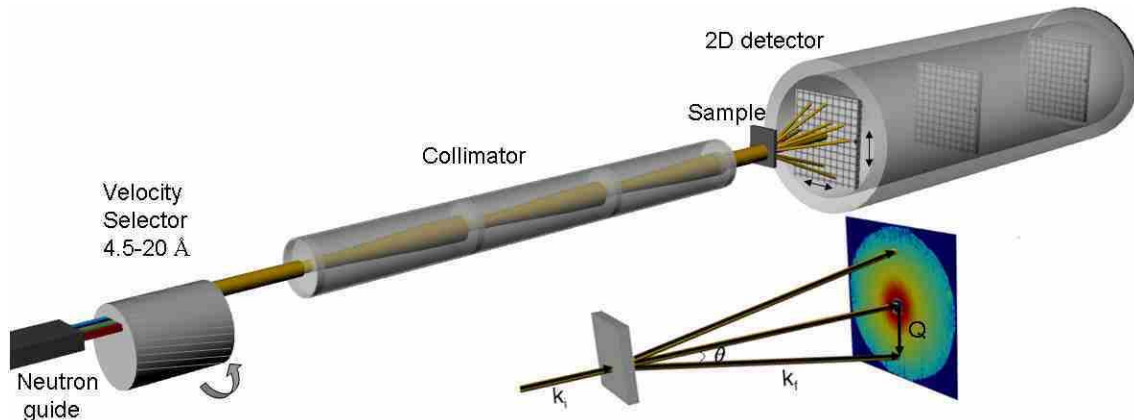


Fig. 2. Experimental set-up of the small angle neutron scattering (SANS) measurements and two dimensional neutron scattering pattern.

A two dimensional neutron scattering pattern is shown in Fig. 2, just below the setup. The 2D scattering patterns resulting from the structure of the sample have been averaged to reach the absolute scattered intensity, $I(Q)$, as a function of the scattering vector, Q .

The small size of the particles characterized using Guinier approximation can be expressed by Eq. (3),

$$\frac{d\Sigma}{d\Omega}(Q) = \frac{d\Sigma}{d\Omega}(0) \exp(-Q^2 R_g^2 / 3), \quad (3)$$

where R_g is the radius of gyration of the particle [6]. The experimental results obtained from SANS measurements were analysed in terms of the Guinier approximation to establish the radius of gyration describing the size of the particles.

The radius of gyration of the sample can be related to characterization for a sphere shape of radius. This spherical structure with radius R is given by Eq. (4),

$$R_g^2 = \int_0^R \gamma(r) r^4 dr \Big/ 2 \int_0^R \gamma(r) r^2 dr = (3/5) R^2, \quad (4)$$

where r is the distance from the sphere centre, R is the maximum extension of the particle, $\gamma(r) = 1$ for a sphere. The sphere radius can be easily calculated from Eq. (4) as $R_g^2 = (3/5) R^2$ and this radius is related to the pore structure of the sample [7].

Three different composites were heat-treated in a furnace at 1300, 1400 and 1500 °C for 5 hours in air atmosphere. The heating and cooling rate was set as 10 °C/min. One composite was measured three different instrument configurations (sample-to-detector distance 1.2, 4 and 6 m) afterwards the same composite was heat treated up to 1300 °C and measured again under identical measurement conditions. Fig. 3 shows the resulting scattering curve of the composite before and after heat treatment. The scattering data possess more than one Guinier region; therefore two different radius of gyration was calculated

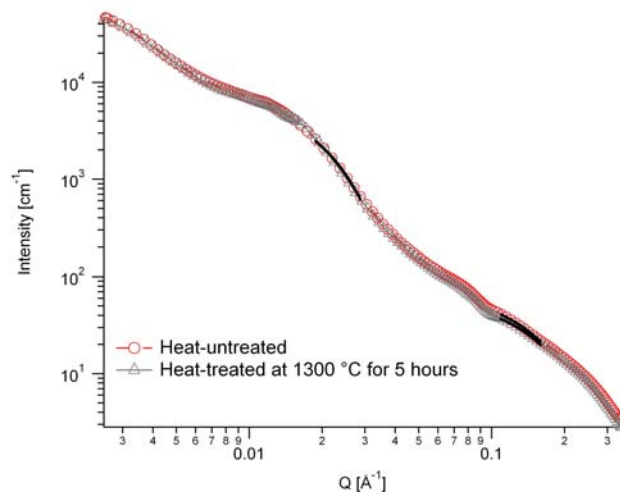


Fig. 3. Scattering curve of the composite before and after heat treatment (1300 °C)

It is clearly seen in Fig.3 that there is no significant pore size change was observed from the scattering pattern in the whole Q-region. From two different Guinier fits, the pore sizes in the small Q-region (0.02-0.03 Å) were calculated as 2.3 nm and in the large Q-region (0.10-0.16 Å) as 1.5 nm.

Difference between untreated and heat-treated at 1400 °C composite was only taken place at high scattering vector over $Q > 0.1 \text{ \AA}^{-1}$. There are no observable pore size changes in the mesopores (2-50 nm) range of the composite after heat-treatment. The pores size was calculated as 9.9 nm for both measurements in the Q-region between 0.02 and 0.03 Å. But as seen in Fig.4, there are evident variations in the small pore size of the composite at high Q-region, the small pore sizes were increased from 0.8 nm to 1.1 nm.

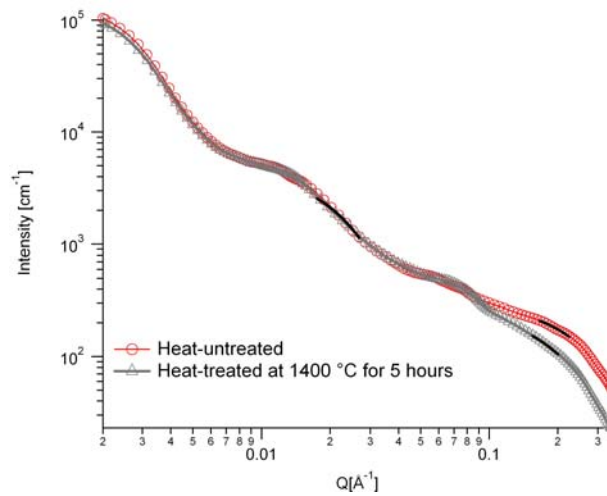


Fig. 4. Scattering curve of the composite before and after heat treatment (1400 °C)

In Fig. 5 the effect of the heat treatment on the scattering pattern can clearly be seen. Micro and macro pore sizes were slightly altered after heat treatment. The pore sizes were increased from 8.5 nm to 9.0 nm and from 1.5 nm to 1.6 nm.

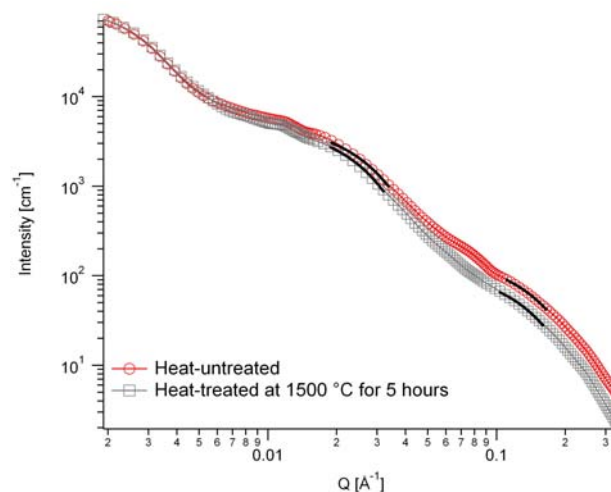


Fig. 5. Scattering curve of the composite before and after heat treatment (1500 °C)

As a result the whole scattering patterns for three different composites show that there is no significant difference micro and macro pore sizes within the composites. Especially at 1300 °C the composite exhibit extremely good stability.

2.2. Cold neutron tomography investigation

Imaging techniques are indispensable tool to visualize the structure, structural change and possible defect within the samples. Neutron imaging method is based on the attenuation of the neutron beam through a sample. The neutron beam penetrates a sample and it is attenuated through the elements within the sample. The transmitted neutrons react with a scintillator (LiZnS) emitting photons. These emitted photons are recorded with a 16-bit cooled very high resolution CCD (Charge Coupled Device) camera having 2048x2048 pixels. Due to the neutron attenuation differences of different elements/isotopes, interior structure of a sample can be visualized.

The macroscopic pore distribution within SiC_f/SiC composite was revealed using non-destructive cold neutron tomography technique. Cold neutrons have an advantage over thermal neutrons because of the cold neutrons interact stronger with the sample and much easily penetrate thick sample. Cold neutron tomography measurements have been performed at the neutron imaging facility CONRAD at the Hahn-Meitner Institute. Cold neutron beam provides wavelength between 2 and 12 Å with a maximum at 3 Å. The beam collimation is expressed by the L/D ratio in which L is the distance between aperture and sample and D is the diameter of the aperture. The image quality is based directly on the beam collimation. SiC_f/SiC composite was investigated at the L/D = 200 ratio and the higher spatial resolution of 200 μm. The neutron flux at the sample position was approximately 10⁷ n/cm²s [8-9].

The tomography reconstruction algorithm was executed Octopus software after that the acquired 3D matrix was visualized by the 3D viewer software VG Studio[®] [10]. Fiber bundles, which consist of ~500-600 fibers, were woven vertical and can be seen in Fig.6a. Fig.6b shows the sidewise pore distribution within the composite. The silicon carbide matrix can not be separated from the silicon carbide fibers because both consist of the same elements. Only segregation of the porosity from the composite has been obtained. The porosity characteristic of the composite can be clearly seen in Fig. 6c and 6d, blue parts in show the porosity distribution within the composite. In 3-dimensional visualization (Fig.6 and 7), the opacity level is changed to highlight the inhomogeneities within the composite.

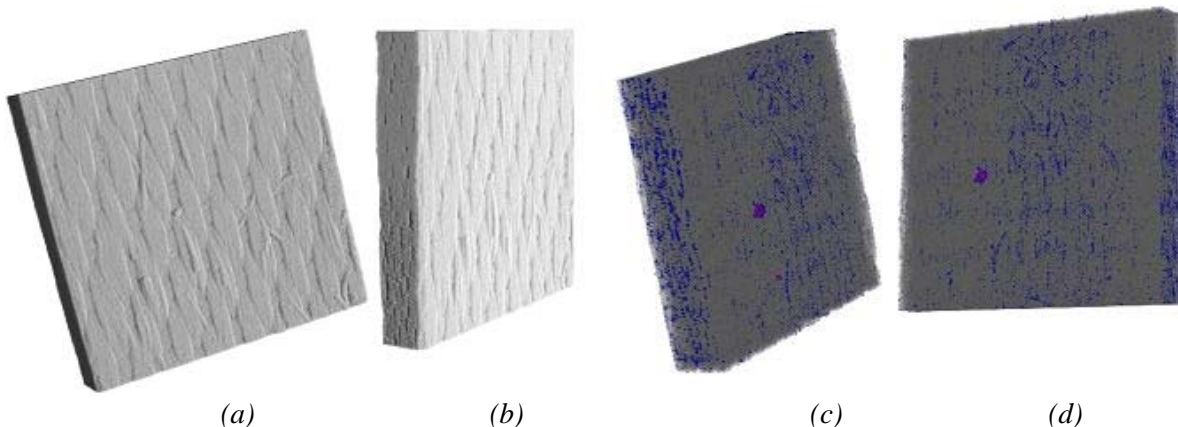


Fig. 6. 3D reconstructed neutron tomography images of the SiC_f/SiC composite with different opacity levels. (a) and (b) images taken without segmentation. (c) and (d) images taken from the different views with segmentation (2 segments being pore and composite).

Most of the pores within the composite are distributed among fiber bundles as seen in Fig.7. Fig. 7 shows also alignment of the fiber bundles in one direction as well as the inhomogeneities (dark spots). Some inhomogeneities are also visible in Fig. 6c and 6d.

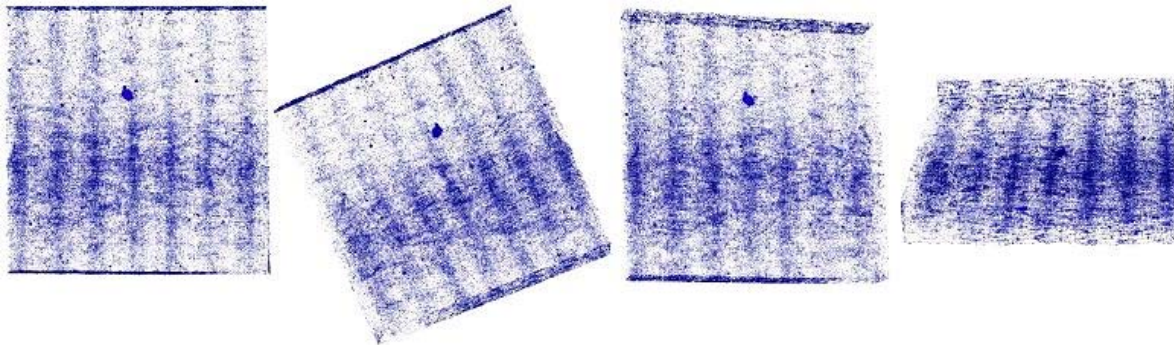


Fig. 7. 3D reconstructed neutron tomography images of the SiC_f/SiC composite from different views.

3. Conclusion

Even SiC/SiC composite is a very weak neutron attenuating sample, neutron tomography and SANS techniques showed a big potential in structure analysis of materials. These techniques are a very effective tool to investigate the inner structure of the materials non-destructively.

SANS measurements display that the pore sizes were partly expanded after the heat-treatment at 1400 and 1500 °C. After the heat-treatment at 1300 °C for 5 hours, the sizes of the pores were not changed significantly. In order to explore the macro-and-nano structure further neutron scattering measurements are needed such as ultra small angle scattering and SANS measurement in the high scattering vector. The pore distribution within the SiC_f/SiC composite was clearly visualized using cold neutron tomography. The porosity within the composite is oriented along the fibre axis.

Acknowledgements

We would like to thank Dr. S. Balog for his technical support during the measurements at the PSI. This work has been supported by European Communities under the contract of Association between EUATOM/ÖAW. The SANS results are based on experiments performed at the Swiss spallation neutron source SINQ, Paul Scherrer Institute, Villigen, Switzerland.

References

- [1] KATOH, Y., et al., "Current status and critical issues for development of SiC composites for fusion applications" *Journal of Nuclear Materials*, 367-370 (2007) 659-671.
- [2] NOZAWA, I., et al., "Recent advances and issues in development of silicon carbide composites for fusion applications", *Journal of Nuclear Materials*, 386-388 (2009) 622-627.
- [3] STRUNZ, P., et al., "In situ SANS study of pore microstructure in YSZ thermal barrier coating", *Acta Materialia*, 52 (2004) 3305-3312.
- [4] STRUNZ, P., et al., "SANS-II at SINQ: installation of the former Riso-SANS facility", *Physica B*, 350 (2004) 783-786.
- [5] BAUER, S. G., "Operation and development of the new spallation neutron source SINQ at the Paul Scherrer Institut", *Nuc. Inst. Met. Phys. Research B* 139 (1998) 65-71.
- [6] GUINIER, A. & FOURNET, G., "Small Angle Scattering of X-ray", NY, John Wiley (1955).

- [7] BEAUCAGE, G., "Particle size distributions from small-angle scattering using global scattering functions", *J. Appl. Cryst.* 37 (2004) 523-535.
- [8] KARDJILOV, N., et al., "Industrial applications at the new cold neutron radiography and tomography facility of the HMI", *Nuc. Inst. Met. Phys. Research A* 542 (2005) 16-21.
- [9] HILGER, A., et al., "The new cold neutron radiography and tomography instrument CONRAD at HMI Berlin", *Physica B*, 385-386 (2006) 1213-1215.
- [10] <http://www.volumegraphics.com/>